Novikov, S.; Lebedeva, N.; Satrapinski, A.; Walden, J.; Davydov, V.; Lebedev, A.

# Graphene based sensor for environmental monitoring of NO2

*Published in:*
Sensors and Actuators B: Chemical

*DOI:*
10.1016/j.snb.2016.05.114

Published: 29/11/2016

*Document Version*
Publisher's PDF, also known as Version of record

Sensors and Actuators B 236 (2016) 1054–1060

Contents lists available at ScienceDirect

Sensors and Actuators B: Chemical

journal homepage: www.elsevier.com/locate/snb

# Graphene based sensor for environmental monitoring of $NO_2$

S. Novikov[a,*], N. Lebedeva[a], A. Satrapinski[b], J. Walden[c], V. Davydov[d], A. Lebedev[d,e]

[a] Department of Micro and Nanosciences, Aalto University, Micronova, Tietotie 3, FI-02150, Espoo, Finland
[b] VTT, Technical Research Centre of Finland, Tekniikantie 1, P.O. Box 9, FI-02151 Espoo, Finland
[c] Finnish Meteorological Institute, Erik Palménin aukio 1, FI-00560 Helsinki, Finland
[d] Ioffe Institute, 26 Politekhnicheskaya, St Petersburg, 194021, Russia
[e] ITMO University, 49 Kronverkskiy prospekt, St.Petersburg, 197101, Russia

ARTICLE INFO

*Article history:*
Received 21 December 2015
Received in revised form 18 May 2016
Accepted 23 May 2016
Available online 24 May 2016

*Keywords:*
Graphene
Gas sensor
Nitrogen dioxide

ABSTRACT

Gas sensor operating in part-per billion (ppb) range is required for environmental monitoring of nitrogen dioxide. Currently there is a lack of cheap sensors, which can operate in this concentration range. In this work, an ultrasensitive gas sensor based on epitaxial graphene on SiC has been proposed. The sensor exhibits a strong and reproducible response to nitrogen dioxide ($NO_2$) for concentrations in air down to 1 ppb. A prototype of a portable device for environmental monitoring which utilizes a combination of sample gas exposure at room temperature and sensor's recovery at elevated temperature has been made. Prototype allows fast and reproducible measurements of $NO_2$ concentration in the typical range for environmental pollution (5 ppb–50 ppb).



## 1. Introduction

Graphene is a two-dimensional monolayer of $sp^2$-hybridized carbon atoms densely packed in a honeycomb crystal lattice. This material has already shown promise as ultrasensitive gas detector. Single layer graphene sensors have every atom at the surface and demonstrate sensitivity down to single molecular level [1]. Their sensitivity is due to their metallic conductivity, even when very few charge carriers are present [2,3]. Thus, changes in number of even a few charge carriers can cause significant changes in sensor response [1]. The high conductivity and few crystal defects of graphene leads to low Johnson [3,4] and thermal switching noise [5]. Graphene mono- or multi-layers for gas sensors can be grown in different ways, for instance, via exfoliation of graphite [1], chemical vapour deposition (CVD) [6,7], reducing of graphite oxide (RGO) [8–10] and epitaxial growth [11,12]. In order to improve the sensing performance of these graphene-based sensors, graphene surface can be modified by conducting polymers [9], metals [13] or patterned into nanostructure mesh [7] or ribbons [14]. Selectivity and sensitivity can be further improved by gating technique [6,8] or by analyzing the low-frequency noise spectra [15,16]. Among other methods of graphene growth, epitaxial graphene has advantages in its application as a gas sensor. Single layer epitaxial graphene is n-type semiconductor naturally due to electron donation from SiC substrate. In [8,11] it was shown that sensors based on n-type graphene exhibit better performance as compared to those based on p-type. CVD and RGO graphene can be also converted into n-type semiconductor, but it requires application of gating technique [8,11] or graphene doping [17]. Epitaxial graphene has also low carrier concentration $5 \times 10^{11} - 10^{12}$ [9], which can be further reduced by exposure of graphene to atmospheric oxygen [18]. In accord sensors based on epitaxial graphene have superior sensitivity, as compared to those based on graphene grown by other methods and show response to measured gas down to sub-ppb range [19].

During the last few years, interest regarding monitoring of air pollutants has grown. Nitrogen monoxide (NO) and nitrogen dioxide ($NO_2$) are harmful air pollutants that have aggressive effects on soil, plants, animals and human health. According to the European Commission air quality standards the $NO_2$ concentration should not exceed the limit of 40 $\mu g/m^3$ at averaging period of one year [20]. From this point of view, it is necessary to develop a highly sensitive and inexpensive $NO_x$ gas sensor that is able to detect low concentrations of NO and $NO_2$ gases. Traditional metal oxide sensors operate in relatively high concentration range 0.1–100 parts per million (ppm) [21], which is not enough for environmental monitoring. Recently, gas sensing experiments have demonstrated that graphene can be an excellent material for $NO_2$ sensors. Graphene layers, grown on SiC, have demonstrated sensitivities down to a parts per billion (ppb) level, and have shown high selectiv-

* Corresponding author.
*E-mail address:* sergey.novikov@aalto.fi (S. Novikov).

http://dx.doi.org/10.1016/j.snb.2016.05.114

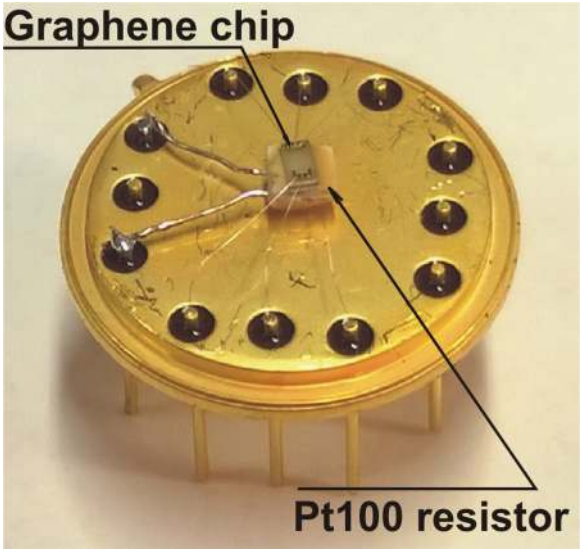


**Fig. 1.** Graphene sensor chip on the holder.

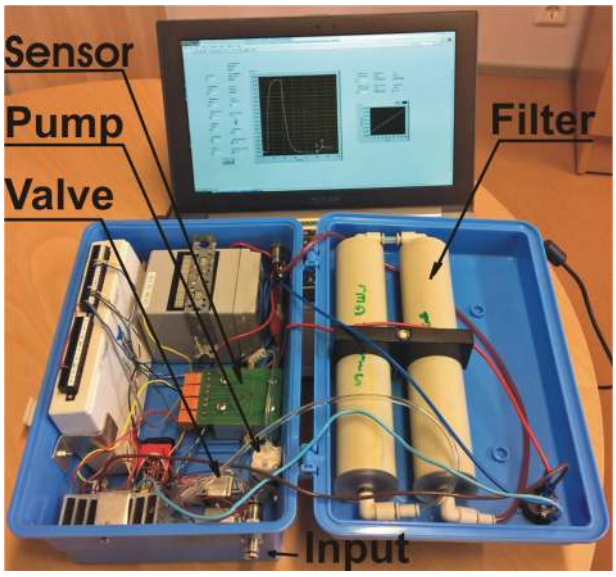


**Fig. 2.** Prototype of portable device for $NO_2$ monitoring.

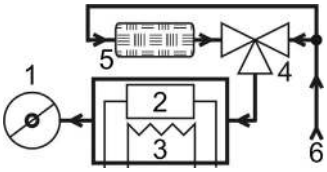


**Fig. 3.** Scheme of the measurement setup.

ity for $NO_2$ detection, with respect to typical interfering gases [6,9,11,15,17].

In the present study, we report on the fabrication of a graphene based sensor and of a measurement device utilizing this graphene sensor, which is suitable for environmental monitoring. We propose a measurement algorithm which allows fast and repeatable measurements of the harmful air pollutants' concentration range down to 1 ppb. The measurement device's selectivity to typical atmospheric contaminants was examined. It was found during the $NO_2$ concentration measurement, that ozone ($O_3$) is the most obstructive component and influences the accuracy of the measurements. A method to distinguish separate responses from ozone and nitrogen dioxide, based on the analysis of desorption rate at elevated temperature, is proposed in this paper.

## 2. Experimental setup and fabrication

Gas sensors were made from the graphene films, grown by the annealing of single crystalline 4H-SiC substrate in Ar ambient at temperature around 1700 °C during a time period close to 5 min. Before the annealing, the substrate was etched at 1600 °C in a 5% $H_2$/95% Ar gas mixture at 1 atm in order to remove scratches available at the surface.

Bar shaped patterns for the sensor were made on the graphene surface of the substrate using laser photolithography over AZ5214 resist. Reactive ion etching in argon and oxygen plasma was used to remove the graphene layer from uncoated areas. An essential property of the graphene based device is its contact resistance at the metal-graphene interface. In order to fabricate stable and low resistance contacts, a two-step metallization process was used. Double layer metal-graphene contacts were made by e-beam evaporation and lift-off photolithography. In both steps, the Ti/Au (5/50 nm) were used. More information concerning contact fabrication was given in [22].

A sensor chip (size 1.5 mm × 1.0 mm) was assembled on a holder, with a Pt100 resistor, which was used as a heater. The design of the sensor (Fig. 1) has low thermal inertia and allows fast thermal cycling. The sensor, along with a sampling system and a computer interface, was assembled into a portable unit suitable for monitoring of $NO_2$ concentration (Fig. 2).

In Fig. 3, a scheme of the measurement setup is presented. The procedure for the measurement of the $NO_2$ gas concentration consists of 3 stages: regeneration, stabilization and exposure to the sample gas. Pump (1) provides the gas flow through the sensor's assembly (2, 3). During regeneration and stabilization, the three-way valve (4) directs the gas flow through the charcoal filter (5) which eliminates nitrogen dioxide and other contaminations. Purified carrier gas is necessary for the successful regeneration of the graphene sensor surface. The desorption rate of nitrogen dioxide from the graphene surface is very low at room temperature. In order to recover the sensor to its initial condition, voltage is applied to Pt100 resistor (3), providing annealing of the sensor (2) at 110 °C before each exposure period. This method significantly increases sensitivity to low nitrogen dioxide concentrations [19]. During stabilization sensors is cooling down to temperature about 25 °C, after that exposure takes place at the same temperature. At the time of exposure, the three-way valve replaces purified gas with a sample gas (6). During the time intervals between the measurements, the sensor is isolated from the external ambient. Since the sensor is mainly operated at temperature near the room temperature, it has low power consumption.

Gas mixtures containing $NO_2$ were prepared by Sonimix 600A gas dilutor manufactured by LN-Industries. Verification has been performed with Apna 360 Horiba Scientific chemiluminescence analyzer. Artificial air has been used as a carrier gas. For measurements of the sensor response to other gases, besides $NO_2$ gas, a custom made gas system was used. A sample gas or liquid was mixed with dry (relative humidity $\phi = 0.02\%$ at 20 °C) or humid air (ambient air purified with a help of a cold trap) by utilizing a two stage dilution system based on mass flow controllers (Aera FC-D980). The dilution ratio can be varied in the range 1:1–1:$10^5$, providing an output concentration in the range of 0.01 ppb–10 ppm. Response, $r$, was expressed as a percentage, %, and defined as the relative change of the sample's resistance under exposure to the gas, $r = (R - R_o)/R_o$, where $R$ is the resistance when the gas is applied,

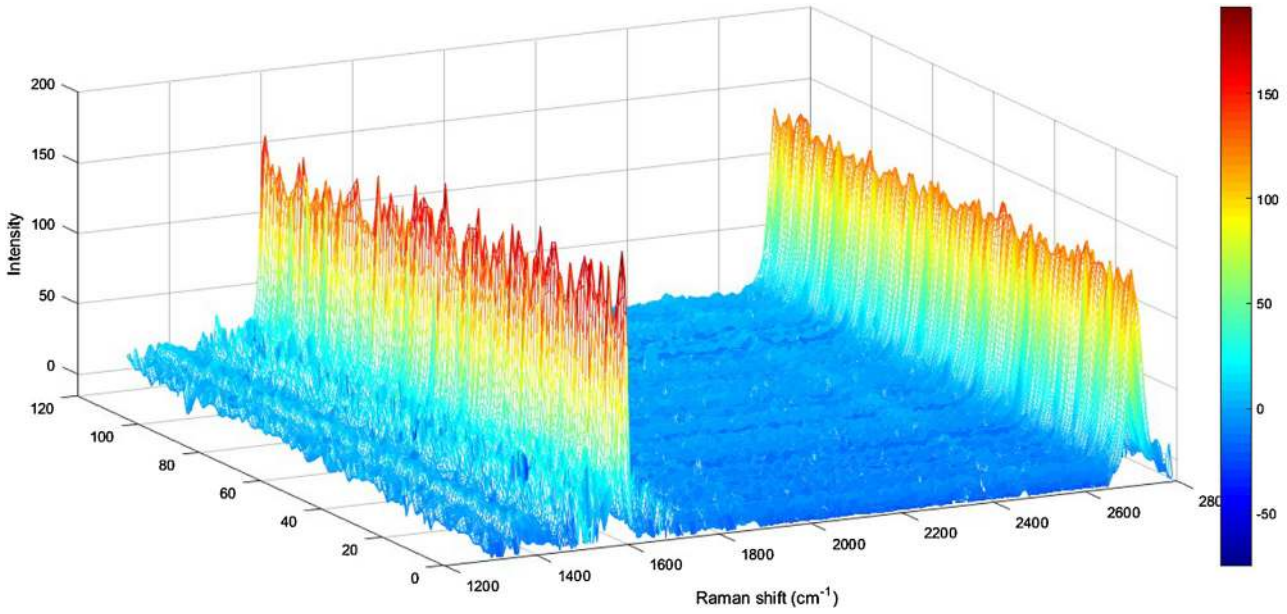


**Fig. 4.** Typical Raman spectra of 10 × 10 μm of the graphene film. SiC background is subtracted. The intensity of the Raman spectra (arb. units) is indicated at the right side of the map.

and $R_0$ is the resistance of the graphene film under the initial conditions defined by the flow of the incoming air.

## 3. Results and discussion

### 3.1. Graphene characterization

Micro-Raman measurements are performed at room temperature in the backscattering configuration using a Horiba Jobin-Yvon T64000 spectrometer equipped with a confocal microscope. The sample is automatically positioned, and fragments of the graphene film with an area of 10 × 10 μm are studied. The total map of the fragment contains 100 spectra. In the experiments, the wavelength of the excitation radiation is 532 nm, the laser power on the sample is about 2.0 mW, and the spot diameter is about 1 μm.

By way of example, Fig. 4 shows a set of Raman spectra of one fragment of the graphene film. For convenience, the second-order spectrum of the 4H-SiC substrate is subtracted from the original spectra. The analysis of the experimental results yields the small FWHM ~13 $cm^{-1}$ of the *G*-line and the absence of the defect *D*-line

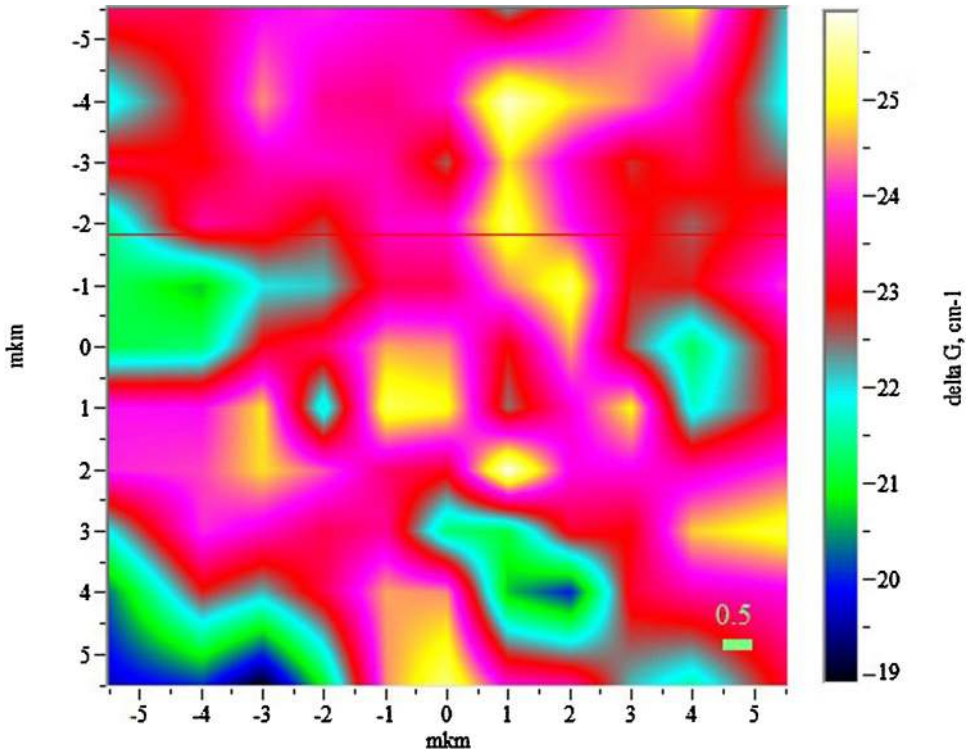


**Fig. 5.** Raman map of G-line shift from 1580 $cm^{-1}$ (ΔG). The value ($cm^{-1}$) of ΔG is indicated at the right side of the map.

that indicates a good crystalline quality of the graphene film. Fig. 4 also shows that the positions of the *G*-lines are blue-shifted relative to a frequency of $\omega_0 = 1580\,cm^{-1}$, which is typical of unstressed crystalline graphite. In the framework of the model of biaxial strain, compression stress σ in the plane of the graphene layer can be estimated using the shift of the *G*-line relative to its position in the Raman spectrum of crystalline graphite [23]:

$$\omega_\sigma - \omega_0 = \alpha\sigma \quad (1)$$

here, $\omega_\sigma$—is the position of the *G*-line in Raman spectrum of graphene on SiC, $\omega_0$—is the position of the *G*-line in Raman spectrum of unstressed graphite, and $\alpha = 7.47\,cm^{-1}/GPa$ is the deformation coefficient of graphite [23]. With the aid of expression (1), the compression stress in the graphene film is estimated as 3.3 GPa, which is significantly higher than usually reported value [23]. In Figs. 5 and 6 the Raman map of *G*-line shift from $1580\,cm^{-1}$ and corresponding histogram are shown, respectively. It is seen that *G*-line shift is relatively uniform in the fragment of the graphene film (a variation is about 10%). It means that a high stress value is a characteristic of the whole graphene film.

Normally, the ratio between intensity of 2D and G lines is used for estimation of graphene film thickness. Resonant Raman process with participation of two phonons is responsible for 2D line. We believe that new conditions for the double resonant for 2D line, appearing under large stress, affect not only the spectral position of 2D line, but also its intensity. Finally, it gives the different ratio between 2D and G lines for unstressed and stressed graphene layers with the similar thickness. In [24], it was claimed that "only unambiguous fingerprint in Raman spectroscopy to identify the number of layers for graphene on SiC (0001) is the line width of the 2D peak". FWHM of 2D Raman peak for our sample is $38\,cm^{-1}$. According to [24], it indicates the existence of single-layer graphene on SiC.

In Fig. 7 Auger spectrum of graphene film is shown. The number of graphene layers on top of SiC was evaluated using method described in [25] and was also found to be about one layer.

I–V characteristic of the sensor is presented in Fig. 8. Current to voltage dependence is almost linear, which is typical for graphene metallic conductivity [2,3].

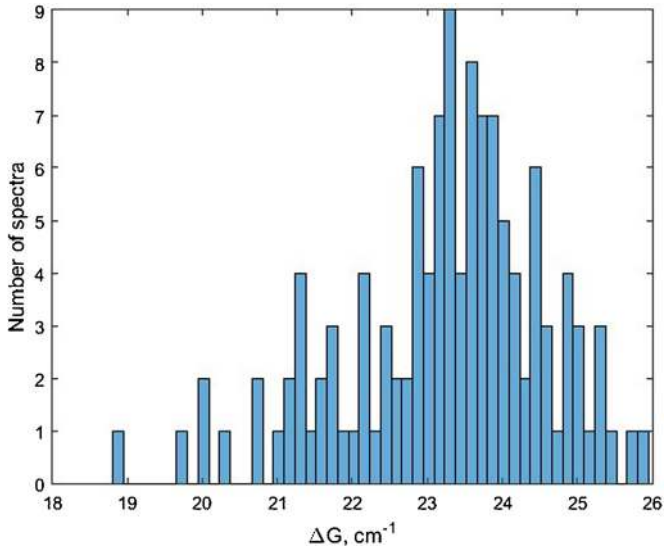


**Fig. 6.** Histogram of the *G*-line shift distribution in the 10 × 10 μm fragment of the graphene film.

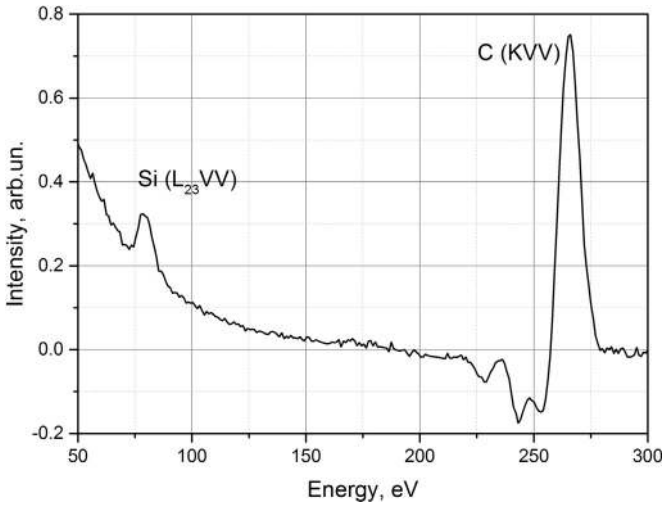


**Fig. 7.** Auger spectrum of the graphene film.

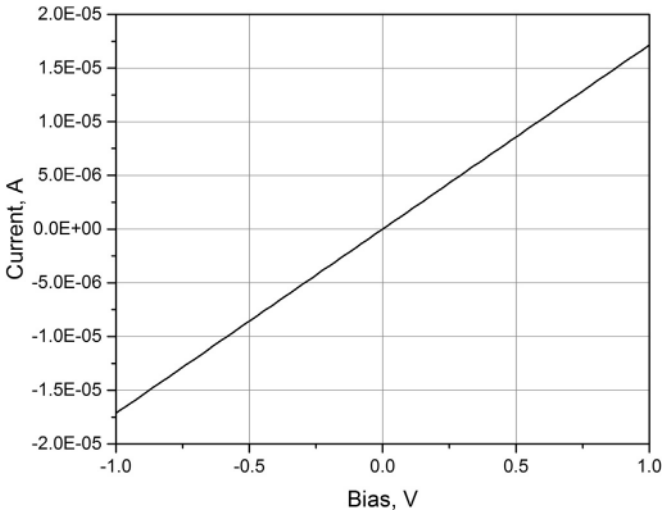


**Fig. 8.** I–V characteristic of graphene based sensor.

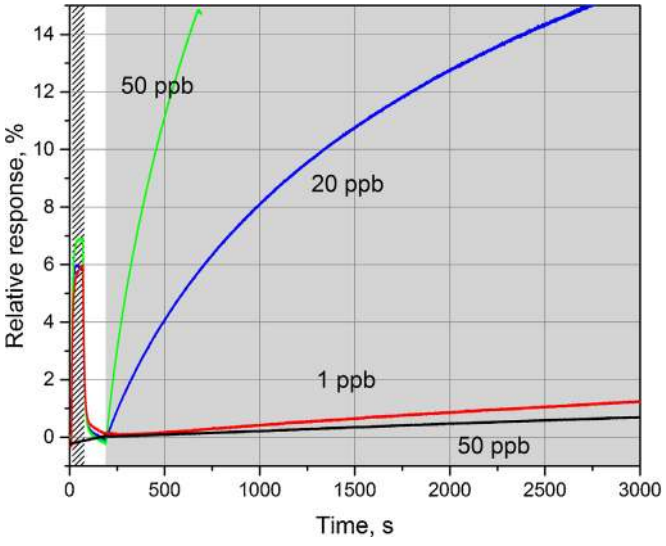


**Fig. 9.** Response on exposure to the gas mixture containing $NO_2$ in concentrations: 1 ppb (red line), 20 ppb (blue line), 50 ppb (green line) and 50 ppb without annealing (black line). Exposure periods are shown as grey band; annealing period is shown as hatched band. (For interpretation of the references to colour in this figure legend, the reader is referred to the web version of this article.)

**Table 1**
$NO_2$ sensors employing graphene active layers grown by different methods.

| Reference | Growth method | Concentration ranges | Response time |
|---|---|---|---|
| [10] | RGO | 0.5–20 ppm | 2500 s |
| [6] | CVD/gating | 20 ppm | 100 s |
| [7] | CVD/nanomesh | 1–10 ppm | 1000 s |
| [17] | RGO/N-doping | 1–10 ppm | 1000 s |
| [12] | epitaxial | 0.5–20 ppm | 200 s |
| [19] | epitaxial | 0.2 ppb–1 ppm | 3000 s |
| This work | epitaxial | 1–50 ppb | 10–3000 s |

### 3.2. Gas sensing performance

In Fig. 9 the response of graphene sensor on exposures to gas mixture, containing $NO_2$ gas in 1 ppb, 20 ppb and 50 ppb concentrations at the room temperature, is presented. $NO_2$ is a strong oxidizer, withdrawing electrons from the surface on which it adsorbs. Therefore, its adsorption on graphene surface is expected to reduce the density of electrons in the case of n-type material, thus leading to the increase in resistivity. Reaction on $NO_2$ concentration as low as 1 ppb is easily recognizable, although for accumulation of 1% in resistivity change requires about one hour of exposure. In Table 1, typical operation ranges for graphene based $NO_2$ sensors grown by different methods are shown. Our sensor works at significantly lower $NO_2$ concentration, than that usually reported [6,7,10,12].

Adsorption can take place ether on low-energy adsorption centers of graphene ($sp^2$–bonded carbon) or on high-energy adsorption centers like oxygen group and defects [26]. In [14] the influence of different kind of defects on performance of graphene-based sensor was studied. It was shown that graphene sensors with liner defects appear to offer superior performance as compared to pristine graphene. According to Raman measurements, graphene layer in our sensor is under stress about 3.3 GPa. Such a high stress is expected to generate linear-type of defects rather than point-type.

We also believe that cleaning of the sensor's surface immediately before sample gas exposure is critically important for obtaining the high sensitivity. In Fig. 9 the response on exposure of 20 ppb $NO_2$ for sensor kept for 1 day under normal room atmosphere is also shown. Response to $NO_2$ of the sensor exposed to room ambient is reduced drastically compared to the pretreated sensor. Moreover, for recovering initial property of the sensor, long annealing in pure carrier gas is required. For fast and reliable operation, sensor has to be separated from the ambient in clean volume except for the measurement time. Such algorithm is realized in the proposed prototype.

Under low $NO_2$ exposure the resistivity of the sensor was increasing approximately linearly with time. At higher exposures response curves started to deviate from the linear law, indicating some saturation [17]. In order to eliminate the effect of saturation and improve linearity of the sensor within the typical measurement cycle, the exposure was interrupted when the responses were changed by 1% from the initial value. Total exposure in this case remains constant for all concentrations. Since the graphene sensor has very high signal to noise ratio [8], this limitation practically did not affect the sensitivity. The sample gas concentration was calculated from the slope of the response curve using linear fitting of the temporal response during sampling time. In Fig. 10 the response of the graphene sensor on short exposures to gas mixture containing $NO_2$ gas (exposure periods are marked as grey bands), in 10 ppb–50 ppb concentration range at the room temperature is presented. Slope of the curves is being proportional to the applied $NO_2$ concentration. In Fig. 11 results of verification of the graphene based gas sensor are presented. In this figure dependence of the data measured by the proposed sensor and by Horiba Scientific gas analyzer for two measurements cycles are presented. The proposed

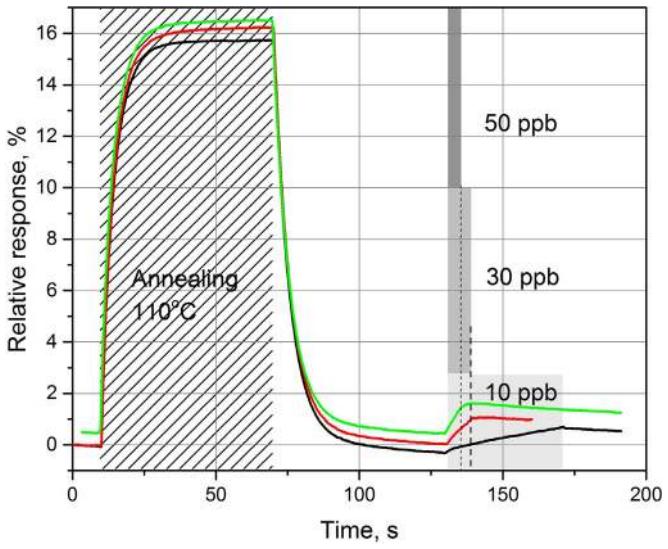


**Fig. 10.** Short measurements of $NO_2$ concentration in air. Exposure periods for 10 ppb (black line), 30 ppb (red line) and 50 ppb (green line) of $NO_2$ are shown as light, medium and dark grey bands. Annealing period is shown as hatched band. Response curves for 30 ppb and 50 ppb are shifted on 0.5% and 1%, respectively, to 10 ppb curve in vertical direction. (For interpretation of the references to colour in this figure legend, the reader is referred to the web version of this article.)

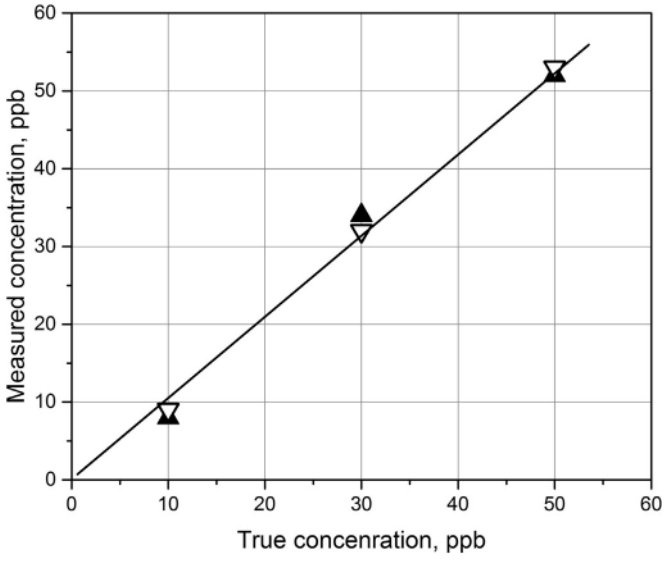


**Fig. 11.** $NO_2$ concentration measured by graphene sensor versus true concentration measured by gas analyzer. Black triangle correspond to the result of the first measurement cycle, white triangles to the second measurement cycle, and the solid line is linear approximation.

device exhibits good linearity and reproducibility for $NO_2$ concentration range, which is typical for environmental monitoring.

### 3.3. Selectivity to other atmospheric contaminants

It is well known that high selectivity towards the target gas is an important characteristic of any high-performance gas sensor. Graphene based sensor, in the same way as other non-functionalized sensors, can have poor cross selectivity with respect to different gases present in the ambient atmosphere. Besides the nitrogen dioxide, the next most significant atmospheric component, affecting graphene based sensor, is the ozone. Its selectivity to $NO_2$ with respect to $O_3$ equals only 2 for the described sensor. Since concentration of ozone in the atmosphere is usually

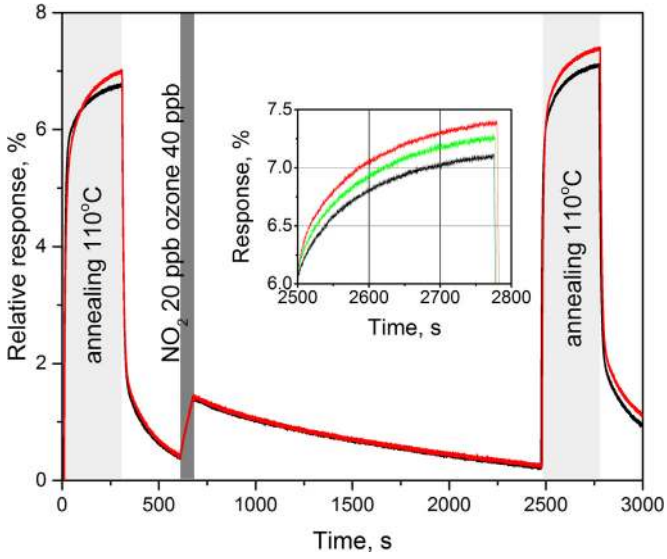


**Fig. 12.** Response on exposure to 20 ppb $NO_2$ (red) and 40 ppb of $O_3$ (black). Exposure periods are shown as grey band, annealing periods as light grey band. On the insert, responses during annealing after exposure to $NO_2$ (red), $NO_2 + O_3$ (green) and $O_3$ (black) are shown. (For interpretation of the references to colour in this figure legend, the reader is referred to the web version of this article.)

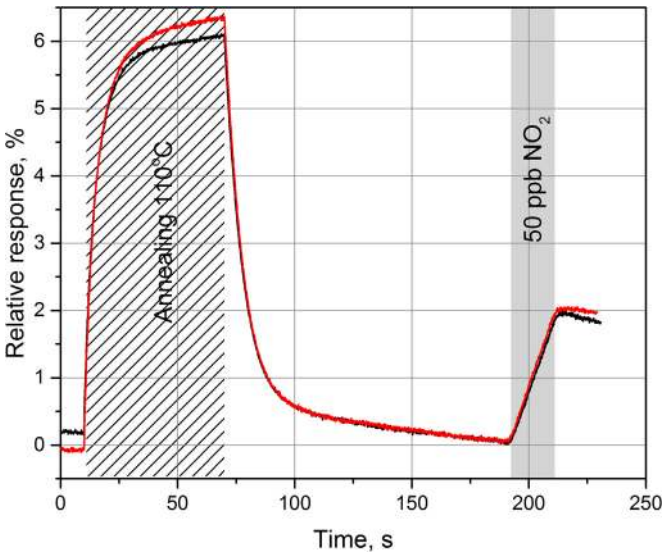


**Fig. 13.** Response on exposure to 50 ppb $NO_2$ at 30%RH (red) and 70%RH (black). Response was measured at the sensor's temperature about 25 °C. Relative humidity was calculated for the temperature 20 °C. Exposure period is shown as grey band; annealing period is shown as hatched band. (For interpretation of the references to colour in this figure legend, the reader is referred to the web version of this article.)

in the same range as that of nitrogen dioxide, a method allowing separation of responses to $NO_2$ and $O_3$ is obviously needed. Oxide based catalysts are commonly used for eliminating ozone from the air before measurements, however, for low concentration range (10–100 ppb) adsorption of $NO_2$ on the catalyst surface significantly distorts the measured concentration and makes the results not applicable. We propose a method for distinguishing responses to $NO_2$ and $O_3$ by analyzing gas desorption rate at elevated temperature. Additional annealing period was added to the measurement run after the period of the gas exposure. Since in our setup the sensor is exposed to the sample gas only until its resistivity is changed by 1%, which corresponds to the same coverage by adsorbed molecules for any gas concentration, resistivity behavior during desorption is assumed to depend on the sample gas composition only. Taking into account, that for our sensor selectivity to $NO_2$ with respect to $O_3$ equals 2, we performed resistivity measurements during desorption after exposure to 20 ppb of $NO_2$ and to 40 ppb of $O_3$, results are presented on Fig. 12. It is clearly seen that response lines for both cases coincide all the time except the desorption periods, where difference is notable. Relative resistivity change after desorption of $NO_2$ is 0,3% larger than that after desorption of $O_3$. This difference is significant compared to 1% resistivity change during exposure period and it reproduces through several measurement cycles. We believe that analyzing the sensor's resistivity changes during annealing (desorption) process can allow separation of contributions from $NO_2$ and $O_3$ in the total response. Unfortunately, due to our hardware limitations, we have not yet tested calibrated gas mixtures containing both nitrogen dioxide and ozone in different concentrations. As a model gas, we used the gas mixture, presumably containing 10 ppb of $NO_2$ and 20 ppb of $O_3$. Resistivity changes during annealing after the exposure to this mixture are presented on the insert together with results for $NO_2$ and $O_3$ (green line) and, as expected, the response line is positioned between those for $NO_2$ and $O_3$.

The main problem that hinders development of a commercially available sensor is a response to the humidity presents in the ambient atmosphere. The response to humidity variation in the carrier gas is shown in Fig. 13. The sensor showed no obvious response to humidity change from 3 to 3000 ppm (0.01–10%RH at 20 °C). In Fig. 14, the response to exposure to 50 ppb of $NO_2$ in two different humidity levels (calculated for 20 °C) is shown. Both curves practically coincide in the exposure time interval. It indicates weak influence of humidity variation on nitrogen dioxide concentration measurement. The sensor was tested to its reaction to acetone, isopropanol and toluene for concentration range up to 100 ppm and did not show any significant response. In Fig. 13 the response on exposure to other important pollutant: ammonia (red line) is also presented. Sensor showed only minor response to 50 ppm of $NH_3$.

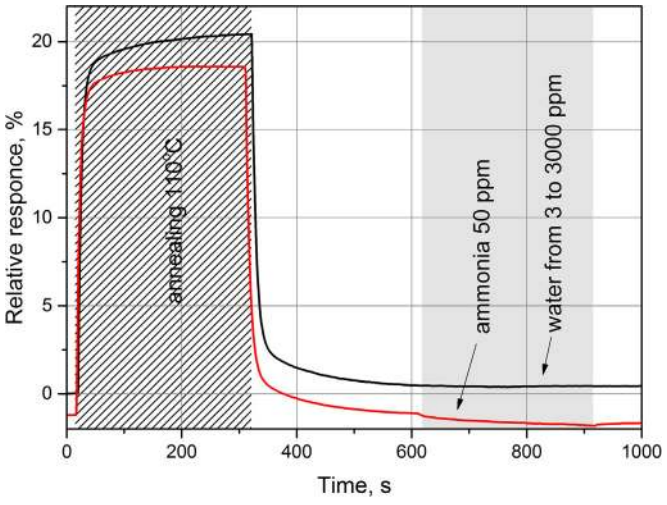


**Fig. 14.** Response on exposure to water vapour (black line) and ammonia (red line). Exposure periods are shown as light grey band, annealing as hatched band. (For interpretation of the references to colour in this figure legend, the reader is referred to the web version of this article.)

## 4. Conclusions

In summary, the graphene-based sensor for environmental monitoring has been made. The measurement device based on proposed sensor shows excellent reproducibility and selectivity with respect to important atmospheric contaminants. Measurement algorithm utilizing analysis of gas desorption from graphene surface at elevated temperature increases selectivity to ozone. The

sensor due to its low cost and low power consumption shows great potential for ultrasensitive detection of $NO_2$.

## Acknowledgment

This research was supported by Nitride Crystals Inc.

## References

[1] F. Schedin, A.K. Geim, S.V. Morozov, E.W. Hill, P. Blake, M.I. Katsnelson, K.S. Novoselov, Detection of individual gas molecules adsorbed on graphene, Nat. Mater. 6 (2007) 652–655.
[2] X. Du, I. Skachko, A. Barker, E.Y. Andrei, Approaching ballistic transport in suspended graphene, Nat. Nano 3 (2008) 491–495.
[3] K.S. Novoselov, A.K. Geim, S.V. Morozov, D. Jiang, M.I. Katsnelson, I.V. Grigorieva, S.V. Dubonos, A.A. Firsov, Two-dimensional gas of massless dirac fermions in graphene, Nature 438 (2005) 197–200.
[4] A.K. Geim, K.S. Novoselov, The rise of graphene, Nat. Mater. 6 (2007) 183–191.
[5] G. Liu, W. Stillman, S. Rumyantsev, Q. Shao, M. Shur, A.A. Balandin, Low-frequency electronic noise in the double-gate single-layer graphene transistors, Appl. Phys. Lett. 95 (2009) 033103.
[6] A.K. Singh, M.A. Uddin, J.T. Tolson, H. Maire-Afeli, N. Sbrockey, G.S. Tompa, M.G. Spencer, T. Vogt, T.S. Sudarshan, G. Koley, Electrically tunable molecular doping of graphene, Appl. Phys. Lett. 102 (2013) 043101.
[7] R. Kanti Paul, S. Badhulika, N.M. Saucedo, A. Mulchandani, Graphene nanomesh as highly sensitive chemiresistor gas sensor, Anal. Chem. 84 (2012) 8171–8178.
[8] G. Lu, K. Yu, L.E. Ocola, J. Chen, Ultrafast room temperature $NH_3$ sensing with positively gated reduced graphene oxide field-effect transistor, Chem. Commun. 47 (2011) 7761–7763.
[9] X. Huang, N. Hu, R. Gao, Y. Yu, Y. Wang, Z. Yang, E. Siu-Wai Kong, H. Weia, Y. Zhang, Reduced graphene oxide–polyaniline hybrid: preparation, characterization and its applications for ammonia gas sensing, J. Mater. Chem. 22 (2012) 22488.
[10] P. Su, H. Shieh, Flexible $NO_2$ sensors fabricated by layer-by-layer covalent anchoring and in situ reduction of graphene oxide, Sens. Actuators B 190 (2014) 865–872.
[11] R. Pearce, T. Iakimov, M. Anderson, L. Hultman, A. Lloid Spetz, R. Yakimova, Epitaxially grown graphene based gas sensors for ultra sensitive $NO_2$ detection, Sens. Actuators B 155 (2011) 451–455.
[12] Md.W.K. Nomania, R. Shishira, M. Qazia, D. Diwana, V.B. Shieldsb, M.G. Spencerb, Gary S. Tompac, Nick M. Sbrockeyc, Goutam Koleya, Highly sensitive and selective detection of $NO_2$ using epitaxial graphene on 6H-SiC, Sens. Actuators B 150 (2010) 301–307.
[13] A. Gut, B. Hsia, A. Sussman, W. Mickelson, A. Zettl, C. Carraroa, R. Maboudian, Graphene decoration with metal nanoparticles: towards easy integration for sensing applications, Nanoscale 4 (2012) 438.
[14] A. Salehi-Khojin, D. Estrada, K.Y. Lin, M. Bae, F. Xiong, E. Pop, R.I. Masel, Polycrystalline graphene ribbons as chemiresistors, Adv. Mater. 24 (2012) 53–57.
[15] S. Rumyantsev, G. Liu, M.S. Shur, R.A. Potyrailo, A.A. Balandin, Selective gas sensing with a single pristine graphene transistor, Nano Lett. 12 (2012) 2294–2298.
[16] S. Rumyantsev, G. Liu, R.A. Potyrailo, A.A. Balandin, M.S. Shur, Selective sensing of individual gases using graphene devices, IEEE Sens. J. 13 (8) (2013) 2818–2822.
[17] F. Niu, J. Liu, L. Tao, W. Wang, W. Song, Nitrogen and silica co-doped graphene nanosheets for $NO_2$ gas sensing, J. Mater. Chem. A 1 (2013) 6130.
[18] P.G. Collins, K. Bradley, M. Ishigami, A. Zettl, Extreme oxygen sensitivity of electronic properties of carbon nanotubes, Science 287 (2000) 1801–1804.
[19] S. Novikov, N. Lebedeva, A. Satrapinski, Ultra-sensitive $NO_2$ gas sensor based on epitaxial graphene, J. Sens. 2015 (2015) 7, http://dx.doi.org/10.1155/2015/108581 (Article ID 108581).
[20] http://ec.europa.eu/environment/air/quality/standards.htm.
[21] A. Afzal, N. Cioffi, L. Sabbatini, L. Torsi, $NO_x$ sensors based on semiconducting metal oxide nanostructures: progress and perspectives, Sens. Actuators B 171–172 (2012) 25–42.
[22] S. Novikov, Joni Hämäläinen, J. Walden, I. Iisakka, N. Lebedeva, A. Satrapinski, Characterization of epitaxial and CVD graphene with double metal-graphene contacts for gas sensing 16th International Congress of Metrology, 13003, (2013). http://cfmetrologie.edpsciences.org/articles/metrology/abs/2013/01/metrology_metr2013_13003/metrology_metr2013_13003.html.
[23] Z.H. Ni, W. Chen, X.F. Fan, J.L. Kuo, T. Yu, A.T.S. Wee, Z.X. Shen, Raman spectroscopy of epitaxial graphene on a SiC substrate, Phys. Rev. B 77 (2008) 115416.
[24] D.S. Lee, C. Riedl, B. Krauss, K. Klitzing, U. Starke, J.H. Smet, Raman spectra of epitaxial graphene on SiC and of epitaxial graphene transferred to $SiO_2$, Nano Lett. 8 (2008) 4320–4325.
[25] E. Vesapuisto, W. Kim, S. Novikov, H. Lipsanen, P. Kuivalainen, Growth temperature dependence of the electrical and structural properties of epitaxial graphene on SiC (0001), Phys. Status Solidi B 248 (8) (2011) 1908–1914.
[26] M.G. Chung, D.H. Kim, H.M. Lee, T. Kim, J.H. Choi, D.K. Seo, J.-B. Yoo, S.-H. Hong, T.J. Kang, Y.H. Kim, Highly sensitive $NO_2$ gas sensor based on ozone treated graphene, Sens. Actuators B 166–167 (2012) 172–176.

## Biographies

**Sergey Novikov** received the Master degree in Physical chemistry from Leningrad Institute of Technology (USSR) in 1982. He obtained his Ph.D from the A. F. Ioffe Institute (St. Petersburg, Russia) in 1994 on the growth and characterization of the alkali-earth fluorides on silicon and gallium arsenide. Since 1995 he is working in the Helsinki University of Technology, where he is currently the senior research scientist. He is a specialist in the field of growth of variety of different materials (graphene, silicon, compound semiconductors, insulators, metals, and metal oxides). Sergey is an author on 77 articles in peer reviewed scientific journals and 42 conference papers.

**Natalia Lebedeva** received her M.Sc. in Physics from St. Petersburg University, Russia in 1998 and Ph.D. in semiconductor technology from Aalto University, Finland in 2013. She is now working in Aalto University as a postdoc scientist and her current research interests include graphene-based devices.

**Alexandre Satrapinski** received his Ph.D. degree in electrical instrumentation engineering from the Institute of Metrology Mendeleev (VNIIM), St. Petersburg, in 1986. He is currently a senior researcher at VTT, Technical Research Centre of Finland Espoo, where he has been working since 1991. His present research interests include the development of the quantum Hall resistance standard and study of the electrical properties of thin film structures at low temperatures.

**Valery Davydov** is currently Head of the Raman spectroscopy team at Ioffe Institute, Russia. He is the author or co-author of more than 150 scientific papers in international journals. His research activity is mainly focused on optical studies of the fundamental physical properties of new semiconductor compounds and related nanostructures.

**Lebedev Alexander** graduate from Optolectronics Department of St Petersburg Electrical Engineering University in 1983. Since 1983 he is working at Ioffe Institute, at the present time (since 1999), in the position of Head of Laboratory «Physics of the semiconductor Devices» and Director of Solid State Electronic Division (since 2014). Since 2004 he began teaching students at St. Petersburg Electrical Engineering University at position of Full Professor. A. A. Lebedev is specialist in technology, physics and device application of Wide band gap semiconductors. Last 10 years Lebedev A. get new results in growth and investigation of graphene films on SiC surface.